Scaling Theory and Morphometrics for a Coarsening Multiscale Surface, via a Principle of Maximal Dissipation

Stephen J. Watson* and Scott A. Norris

Engineering Sciences and Applied Mathematics, Northwestern University, Evanston, Illinois 60208, USA

(Received 30 March 2004; published 4 May 2006)

We consider the coarsening dynamics of multiscale solutions to a dissipative singularly perturbed partial differential equation which models the evolution of a thermodynamically unstable crystalline surface. The late-time leading-order behavior of solutions is identified, through the asymptotic expansion of a maximal-dissipation principle, with a completely faceted surface governed by an intrinsic dynamical system. The properties of the resulting piecewise-affine dynamic surface predict the scaling law $\mathcal{L}_{\mathcal{M}} \sim t^{1/3}$, for the growth in time t of a characteristic morphological length scale $\mathcal{L}_{\mathcal{M}}$. A novel computational geometry tool which directly simulates a million-facet piecewise-affine dynamic surface is also introduced. Our computed data are consistent with the dynamic scaling hypothesis, and we report a variety of associated morphometric scaling functions.

DOI: 10.1103/PhysRevLett.96.176103 PACS numbers: 68.55.−a, 05.70.Ln, 81.10.Aj

The characterization of self-assembled faceted surfaces is a central theoretical challenge in surface science [1], since the ensuing morphological statistics (morphometrics) impact applications in diverse areas. For example, chiral faceted surfaces, obtained from chemisorption of chiral molecules, serve as enantiospecific heterogeneous catalysts, which can then select and/or detect biomolecular enantiomers [2]. Also, the ensemble of faceted nanoscale crystals (quantum dots) that self-assemble during the deposition of SiGe alloys on Si surfaces [3] possess novel optoelectronic properties which depend sensitively on the morphometric structure.

Facets arise for a thermodynamic reason, namely, *nonconvexity* of the surface energy $\sigma(\mathbf{n})$ with respect to the surface normal $\mathbf{n}$ [4]. The spinodal decomposition of a thermodynamically unstable orientation into a faceted surface [1,5] is commonly observed in metals, semiconductors, and ceramics [6–9]; see Fig. 1. Further, upon annealing, or when subject to some form of growth, these faceted morphologies undergo a self-similar coarsening. Various power-law scalings $\mathcal{L}_{\mathcal{M}} \sim t^n$, for the growth in time t of the characteristic morphological length scale $\mathcal{L}_{\mathcal{M}}$ [10–13], as well as scale-invariant surface structure factors [11] have been reported.

Multiscale continuum models governing the entire process of spinodal decomposition through facet coarsening have been derived from first principles, subject to a small facet-slope approximation [14,15]. The coarsening dynamics of such models has been examined through direct simulation [15–18], and power-law scalings consistent with experimental findings were surmised. However, theoretical predictions for the scaling exponent n have remained in a heuristic state, while direct simulations to probe the morphometric structure were previously limited by the multiscale nature of the problem.

In this Letter, we theoretically characterize the leading-order dynamics of a dissipative multiscale continuum model for coarsening faceted crystal surfaces. The theory identifies a dynamical system governing the leading-order purely faceted surface, by utilizing a novel asymptotic maximal-dissipation principle [19]. The properties of the resulting piecewise-affine dynamic surface (PADS) imply the scaling law $\mathcal{L}_{\mathcal{M}} \sim t^{1/3}$, which confirms earlier predictions [16,17]. We also introduce a unique computational geometry tool, which directly simulates a million-facet PADS by explicitly treating all the associated topological and critical events that arise as the surface coarsens. Our computed data reveals dynamic scaling (statistical self-similarity) at all levels of interrogation, and we report here on the scale-invariant distributions for n-sided facets and the relative facet area.

The free energy of a faceted crystalline surface $z = h(x, y)$ has been modeled, in the small-slope limit, by the projected-area ($dA = dxdy$) integral

$$E[h] := \int \left[W(\nabla h) + \frac{1}{2}\varepsilon^2 (\Delta h)^2 \right] dA; \qquad (1)$$

$W(\nabla h)$ is a nonconvex function of the slope, $\nabla h = h_x \mathbf{i} + h_y \mathbf{j} = p\mathbf{i} + q\mathbf{j}$, while $0 < \varepsilon \ll 1$ is a dimensionless con-

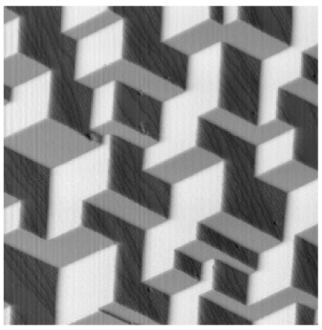

FIG. 1. Scanning electron microscope image of a faceted CuO_2 surface exhibiting threefold symmetry [25].

stant, and $\Delta = (\partial^2/\partial x^2) + (\partial^2/\partial y^2)$. Furthermore, attachment-kinetics limited crystal growth is modeled [14,15] by the dissipative evolution equation $\frac{\partial h}{\partial t} = -\frac{\delta E}{\delta h}$, where $\frac{\delta E}{\delta h}$ denotes the variational derivative (L^2 gradient) of E; i.e.,

$$\frac{\partial h}{\partial t} = \frac{\partial}{\partial x}\left[\frac{\partial W}{\partial p}(\nabla h)\right] + \frac{\partial}{\partial y}\left[\frac{\partial W}{\partial q}(\nabla h)\right] - \varepsilon^2\Delta^2 h. \quad (2)$$

We consider here the trigonally symmetric potential

$$W(p, q) := -\tfrac{1}{6}(q^2 + p^2) + \tfrac{1}{9}(q^3 - 3qp^2) + \tfrac{1}{6}(q^2 + p^2)^2,$$

which is minimized by the gradients $\mathbf{m} = p\mathbf{i} + q\mathbf{j} \in \mathcal{G}$,

$$\mathcal{G} := \left\{\frac{\sqrt{3}}{2}\mathbf{i} + \frac{1}{2}\mathbf{j}, -\frac{\sqrt{3}}{2}\mathbf{i} + \frac{1}{2}\mathbf{j}, -\mathbf{j}\right\}. \quad (3)$$

Numerical simulations of (2) reveal that solutions display two disparate length scales at late times [16]; see Fig. 2. The outer scale arises from the $O(1)$-size domains wherein the gradient ∇h is approximately equal to a particular $\mathbf{m} \in \mathcal{G}$. At the same time, the $O(\varepsilon)$-width boundary layer (*diffuse edge*), residing between adjacent outer-scale domains and wherein an interpolation between two different $\mathbf{m} \in \mathcal{G}$ occurs, provides the inner scale. The outer-scale structure of the solution surface $z = h$ is therefore approximated, to leading order, by the piecewise-affine surface $z = \mathcal{H}$: i.e.,

$$h = \mathcal{H} + O(\varepsilon), \quad \text{where } \nabla\mathcal{H} \in \mathcal{G}. \quad (4)$$

Further, the projected-edge set $\mathcal{E}_{\mathcal{H}}$, obtained by projecting the edges of the surface $z = \mathcal{H}$ onto the plane $z = 0$, outlines the diffuse-edge network associated with h.

The free energy $E[h]$ concentrates, as a result of (4), into an $O(\varepsilon)$-width boundary layer centered on $\mathcal{E}_{\mathcal{H}}$. More precisely, the inner-scale structure of ∇h around $\mathcal{E}_{\mathcal{H}}$ induces an effective line-energy density $\gamma\varepsilon$ on $\mathcal{E}_{\mathcal{H}}$, where $\gamma := \int_{-\sqrt{3}/2}^{\sqrt{3}/2}\sqrt{W(p, -1/2)}dp = \sqrt{3}/2$ [16]. However, since $W(\mathbf{m}) = 0$ and $\frac{\partial W}{\partial p}(\mathbf{m}) = 0 = \frac{\partial W}{\partial q}(\mathbf{m})$ for all $\mathbf{m} \in \mathcal{G}$, an examination of the Taylor expansion of $E[h]$ reveals an outer-scale contribution of at most $O(\varepsilon^2)$. We therefore obtain the asymptotic expansion

$$E[h] = \mathcal{P}[\mathcal{H}]\gamma\varepsilon + O(\varepsilon^2), \quad (5)$$

where $\mathcal{P}[\mathcal{H}]$ denotes the total length (perimeter) of $\mathcal{E}_{\mathcal{H}}$. Furthermore, the slow time scale $\tau := \gamma\varepsilon t$ on which solutions of (2) evolve at late times is naturally identified:

$$\frac{\partial h}{\partial \tau} = -\frac{1}{\gamma\varepsilon}\frac{\delta E}{\delta h}. \quad (6)$$

The gradient constraint $\nabla\mathcal{H} \in \mathcal{G}$ greatly simplifies the kinematics of the faceted surface $z = \mathcal{H}(x, y, \tau)$, since it implies each facet may only move with a fixed orientation; we presume nucleation of new facets is precluded. It follows that the sole degree of freedom of the ith facet, $i \in I$, is a displacement in height, parametrized through a local height coordinate $\mathcal{H}_i$: *Edges* and triple junctions of the surface offer no constraint, assuming no topology change, with their positions following the locus of intersection of the two and three intersecting facets which comprise them. Hence, the kinematics of $z = \mathcal{H}$ are captured by specifying the instantaneous vertical velocity $\mathcal{V}_i = d\mathcal{H}_i/d\tau$ of each facet. Further, from (4) we deduce the asymptotic form of the solution velocity h_τ:

$$\frac{\partial h}{\partial \tau} = \sum_{i\in I}\frac{d\mathcal{H}_i}{d\tau}\chi_{\mathcal{F}_i} + O(\varepsilon), \quad (7)$$

where the set $\mathcal{F}_i$ coincides with the projection of the ith facet onto the plane $z = 0$, while $\chi_{\mathcal{F}_i}$ denotes the characteristic function which takes the values 1 and 0 on and off the set $\mathcal{F}_i$, respectively.

To identify the dynamical system governing the leading-order purely faceted surface $z = \mathcal{H}$ requires a method which connects the outer-scale kinematics of h, namely, (7), with the inner-scale edge network on which the energy essentially resides, as expressed by (5). As in Ref. [19], the asymptotic expansion in ε of an Onsager-Raleigh-type principle of maximal *dissipation* [20] will provide the requisite link, as we shall now demonstrate.

First, the *dissipation* of a virtual velocity $v(x, y)$ is, by definition, $\int v^2 dA$. Now a simple computation shows that the (scaled) *power* of a solution to (6), namely,

$$\frac{1}{\gamma\varepsilon}\frac{d}{d\tau}E[h] = \int\frac{1}{\gamma\varepsilon}\frac{\delta E}{\delta h}\frac{\partial h}{\partial \tau}dA, \quad (8)$$

balances the dissipation of h_τ according to

$$\int\frac{1}{\gamma\varepsilon}\frac{\delta E}{\delta h}\frac{\partial h}{\partial \tau}dA + \int\left(\frac{\partial h}{\partial \tau}\right)^2 dA = 0. \quad (9)$$

Replacing h_τ in (9) by v, we identify the class $\mathcal{C}_\varepsilon$ of power-dissipation compatible virtual velocities; i.e.,

$$\mathcal{C}_\varepsilon := \left\{v: \int v^2 dA + \int\frac{1}{\gamma\varepsilon}\frac{\delta E}{\delta h}v dA = 0\right\}. \quad (10)$$

Further, a direct calculation shows that for any $v \in \mathcal{C}_\varepsilon$

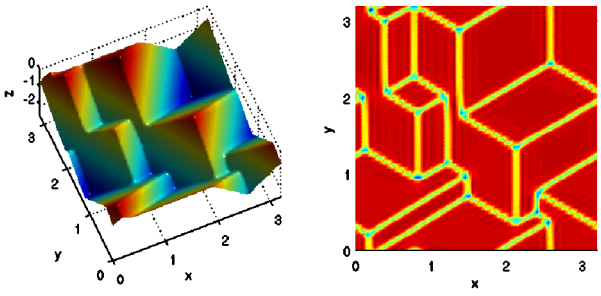

FIG. 2 (color online). Representative late-time surface profile $z = h(x, y, t)$ from a numerical simulation of (2), alongside a gray-scaled distribution of the gradient magnitude $m = |\nabla h(x, y)|$; $m = 1$ (dark), $m = 1/2$ (light).

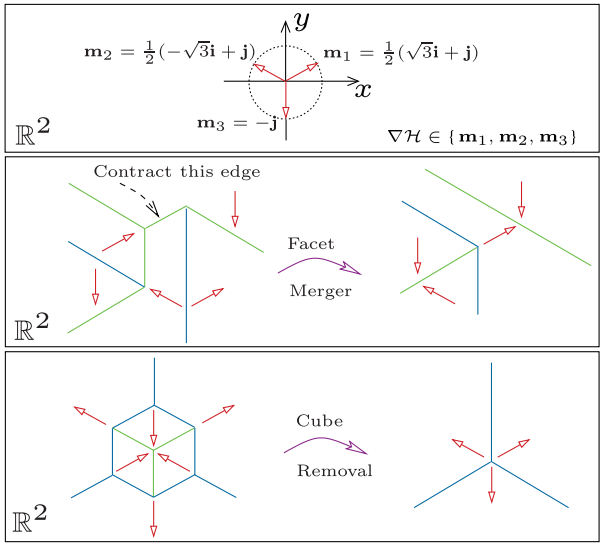

FIG. 3 (color). Schematics of two possible topological or critical events that may arise during the evolution of a piecewise-affine $\mathcal{H}$.

$$\int v^2 dA = \int \left(\frac{1}{\gamma\varepsilon}\frac{\delta E}{\delta h}\right)^2 dA - \int \left(v + \frac{1}{\gamma\varepsilon}\frac{\delta E}{\delta h}\right)^2 dA.$$

Hence, h_τ maximizes the dissipation among all virtual velocities $v \in \mathcal{C}_\varepsilon$. Indeed, one may readily show that the *principle of maximal dissipation*, which states

$$\frac{\partial h}{\partial \tau} \in \mathcal{C}_\varepsilon \tag{11a}$$

$$\text{and} \qquad \int \left(\frac{\partial h}{\partial \tau}\right)^2 dA = \max_{v \in \mathcal{C}_\varepsilon} \int v^2 dA, \tag{11b}$$

is both a necessary and sufficient condition for (6).

We now develop the asymptotic expansion (11) with respect to ε. We begin by observing that (7) implies

$$\int \left(\frac{\partial h}{\partial \tau}\right)^2 dA = \sum_{i \in I} \mathcal{A}_i \left(\frac{d\mathcal{H}_i}{d\tau}\right)^2 + O(\varepsilon), \tag{12}$$

where $\mathcal{A}_i$ denotes the area of $\mathcal{F}_i$. Also, recalling (8) and then applying (5), one concludes

$$\begin{aligned} \frac{1}{\gamma\varepsilon}\int \frac{\delta E}{\delta h}\frac{\partial h}{\partial \tau} dA &= \frac{d}{d\tau}\mathcal{P}[\mathcal{H}] + O(\varepsilon) \\ &= \sum_{i \in I} \frac{\partial \mathcal{P}}{\partial \mathcal{H}_i}\frac{d\mathcal{H}_i}{d\tau} + O(\varepsilon). \end{aligned} \tag{13}$$

Utilizing both (12) and (13), we may expand (9) or, equivalently, (11a) to deduce, upon equating $O(1)$ terms,

$$\sum_{i \in I} \mathcal{A}_i \left(\frac{d\mathcal{H}_i}{d\tau}\right)^2 + \sum_{i \in I} \frac{\partial \mathcal{P}}{\partial \mathcal{H}_i}\frac{d\mathcal{H}_i}{d\tau} = 0. \tag{14}$$

Since (7) also implies that any virtual velocity of h takes the asymptotic form $v = \sum_{i \in I} \chi_{\mathcal{F}_i} \mathcal{V}_i + O(\varepsilon)$, we similarly find that $v \in \mathcal{C}_\varepsilon$ precisely when $\mathcal{V} := (\mathcal{V}_i)_{i \in I} \in \mathcal{C}_0$, where

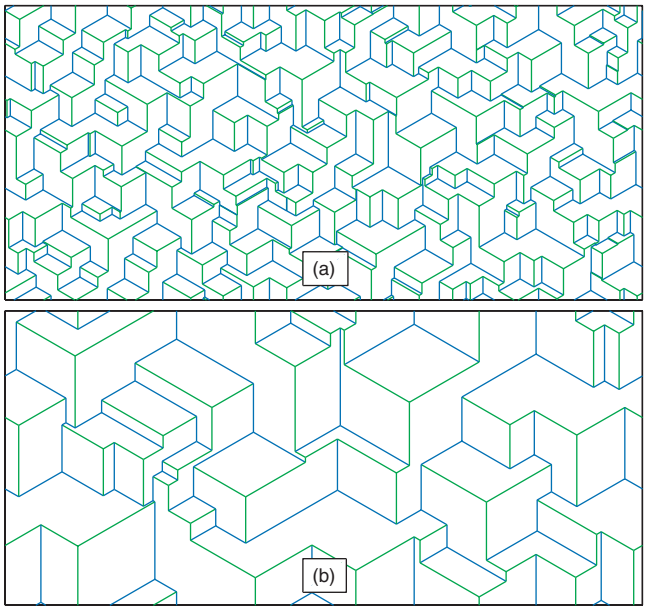

FIG. 4 (color). (a) *Early* and (b) *late*-time surface morphologies from a PAGE simulation of a PADS governed by (18).

$$\mathcal{C}_0 := \left\{ \mathcal{V} : \sum_{i \in I} \mathcal{A}_i \mathcal{V}_i^2 + \sum_{i \in I} \frac{\partial \mathcal{P}}{\partial \mathcal{H}_i} \mathcal{V}_i = 0 \right\}. \tag{15}$$

From this fact, we deduce the asymptotic expansion

$$\max_{v \in \mathcal{C}_\varepsilon} \int v^2 dA = \max_{\mathcal{V} \in \mathcal{C}_0} \sum_{i \in I} \mathcal{A}_i \mathcal{V}_i^2 + O(\varepsilon). \tag{16}$$

Finally, using both (12) and (16) in (11b) and equating $O(1)$ terms, and also noting (14) and (15), we deduce the asymptotic form of (11), namely,

$$\left(\frac{d\mathcal{H}_i}{d\tau}\right)_{i \in I} \in \mathcal{C}_0 \tag{17a}$$

$$\text{and} \qquad \sum_{i \in I} \mathcal{A}_i \left(\frac{d\mathcal{H}_i}{d\tau}\right)^2 = \max_{\mathcal{V} \in \mathcal{C}_0} \sum_{i \in I} \mathcal{A}_i \mathcal{V}_i^2. \tag{17b}$$

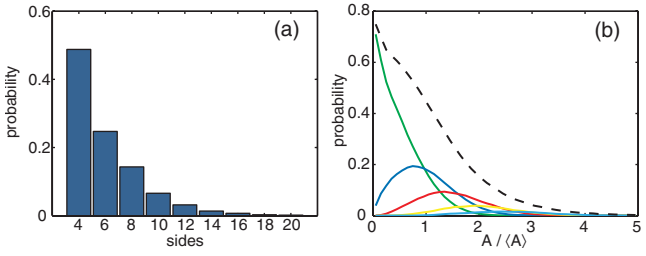

FIG. 5 (color). (a) Scale-invariant histogram of relative frequency of $2n$-sided facets. (b) Scale-invariant distribution of dimensionless facet areas $\rho(A/\langle A\rangle)$ (dashed line) and its decomposition into $2n$-sided facets; $n = 2$ (green), $n = 3$ (dark blue), $n = 4$ (red), $n = 5$ (yellow), and $n = 6$ (light blue).

Hence, $(d\mathcal{H}_i/d\tau)_{i\in I}$ maximizes the *asymptotic dissipation* $\sum_{i\in I}\mathcal{A}_i\mathcal{V}_i^2$ among all virtual velocities $\mathcal{V}\in\mathcal{C}_0$. Furthermore, it is readily shown that (17) is equivalent to

$$\frac{d\mathcal{H}_i}{d\tau} = -\frac{1}{\mathcal{A}_i}\frac{\partial\mathcal{P}}{\partial\mathcal{H}_i}, \tag{18}$$

a dynamical system which intrinsically and uniquely determines the evolution of the faceted surface $z=\mathcal{H}$.

The *piecewise-affine dynamic surface* (PADS) governed by (18) preserves the dissipative structure of the underlying model Eq. (6); the ith facet is acted on by the driving force $-\partial\mathcal{P}/\partial\mathcal{H}_i$ and possesses an effective mobility inversely proportional its projected area. In particular, the perimeter of the projected-edge set $\mathcal{P}[\mathcal{H}]$ must decrease as the surface evolves. Furthermore, discontinuous decreases in perimeter may arise during topological or critical events such as those represented in Fig. 3.

The dynamic scaling hypothesis asserts that the spatial surface statistics of a coarsening PADS are temporally invariant upon rescaling space by a suitable characteristic morphological length scale $\mathcal{L}_{\mathcal{M}}(\tau)$. Assuming such statistical self-similarity, the invariance of (18) under the spatiotemporal scaling $L\to\lambda L$ and $\tau\to\lambda^3\tau$ implies the power-law scaling $\mathcal{L}_{\mathcal{M}}(\tau)\sim\tau^{1/3}$.

We have developed a novel computational geometry tool, the piecewise-affine-geometry evolver (PAGE), to simulate a PADS possessing a statistically significant number of facets; see Fig. 4. It is based on the planar-graph structure (facet, edge, or vertex) of a piecewise-affine surface. Further, it treats all the topological and critical events that emerge during coarsening by a theoretically based graph-rewriting algorithm; here the topological complexity exceeds that of the previously studied 2D coarsening networks associated with foams and polycrystals [21]. We present in Fig. 5 a brief sample of our computed statistics, derived from averaging the data from 20 independent PAGE simulations of a PADS starting with 25 000 facets. After an initial transient, associated with but insensitive to the initial data, we find the scaling law $\sqrt{\langle\mathcal{A}_i\rangle}=1.75\tau^{0.33}$; $\sqrt{\langle\mathcal{A}_i\rangle}$ denotes the square root of the average projected facet area. This is not only consistent with our theoretically predicted scaling exponent $n=1/3$ but also reflects the fine details of the coarsening pathway through the experimentally important prefactor 1.75 [22]. In Fig. 5, we report on some scale-invariant morphometric measures which further support the dynamic scaling hypothesis.

In conclusion, a novel asymptotic expansion of a generalized Onsager-Raleigh maximal-dissipation principle [19], in conjunction with a unique computational geometry tool—PAGE—provide a comprehensive morphometric characterization of multiscale solutions to a continuum model for thermodynamically unstable crystalline surfaces. The theoretical expansion method, which itself applies to any singularly perturbed gradient descent [19], identifies the late-time large-scale behavior of solutions with a completely faceted surface governed by an intrinsic dynamical system, a so-called PADS. The scaling properties of this approximating PADS predict a coarsening law which is consistent with direct numerical simulations of the original model. Furthermore, data taken from PAGE simulations of a million-facet PADS confirm statistical self-similarity of the ensuing morphology, and we report on the observed scale-invariant distributions for $2n$-sided facets and the relative facet area. Comparisons of our fine-scale morphometric predictions with detailed data from *in situ* spectroscopy and microscopy may serve as a useful and robust model-validation probe. Last, lying at the intersection between nonequilibrium statistical mechanics and complex networks [23], this coarsening PADS, and others like it [24], are complex systems whose emergent behavior warrants further study.

This research was primarily supported by NSF DMS-0309709 and partially by NASA NAG3-2369. S. J. W. acknowledges partial support from NSF 0102794 and SFB-611 sponsored visits to the University of Bonn.

*Corresponding author.
Electronic address: s-watson@northwestern.edu

[1] E. D. Williams and N. C. Bartelt, Science **251**, 393 (1991).
[2] J. A. Switzer *et al.*, Nature (London) **425**, 490 (2003).
[3] A. Rastelli *et al.*, Phys. Rev. Lett. **95**, 026103 (2005).
[4] C. Herring, Phys. Rev. **82**, 87 (1951).
[5] J. W. Cahn, Acta Metall. **10**, 179 (1962).
[6] W. W. Mullins, Philos. Mag. **6**, 1313 (1961).
[7] D. Knoppik and A. Losch, J. Cryst. Growth **34**, 332 (1976).
[8] J. Heffelfinger and C. Carter, Surf. Sci. **389**, 188 (1997).
[9] N. Reinecke and E. Taglauer, Surf. Sci. **454**, 94 (2000).
[10] J. A. Stroscio *et al.*, Phys. Rev. Lett. **75**, 4246 (1995).
[11] S. Song *et al.*, Phys. Rev. Lett. **74**, 5240 (1995).
[12] K. J. Caspersen *et al.*, Phys. Rev. B **65**, 193407 (2002).
[13] A. C. Durr *et al.*, Phys. Rev. Lett. **90**, 016104 (2003).
[14] J. Stewart and N. Goldenfeld, Phys. Rev. A **46**, 6505 (1992).
[15] F. Liu and H. Metiu, Phys. Rev. B **48**, 5808 (1993).
[16] M. Siegert, Phys. Rev. Lett. **81**, 5481 (1998).
[17] D. Moldovan and L. Golubovic, Phys. Rev. E **61**, 6190 (2000).
[18] P. Smilauer *et al.*, Phys. Rev. E **59**, R6263 (1999).
[19] S. J. Watson (unpublished).
[20] L. Onsager, Phys. Rev. **38**, 2265 (1931).
[21] G. Schliecker, Adv. Phys. **51**, 1319 (2002).
[22] J. Krug, Physica (Amsterdam) **340A**, 647 (2004).
[23] A. L. Barabasi and R. Albert, Science **286**, 509 (1999).
[24] S. J. Watson *et al.*, Physica (Amsterdam) **178D**, 127 (2003).
[25] Courtesy of Edmund Taglauer.